

Received: 2019.04.08  
Accepted: 2019.05.07  
Published: 2019.07.12

## Two GEO MicroRNA Expression Profile Based High-Throughput Screen to Identify MicroRNA-31-3p Regulating Growth of Medullary Thyroid Carcinoma Cell by Targeting RASA2

Authors' Contribution:  
Study Design A  
Data Collection B  
Statistical Analysis C  
Data Interpretation D  
Manuscript Preparation E  
Literature Search F  
Funds Collection G

ABCDEF G 1 **Mei Jiang\***  
BDF 2 **Xin Shi\***  
CF 3 **Hua Zhu**  
ABCDEF G 4 **Wu Wei**  
BC 5 **Jinyan Li**

1 Department of Radiology, Shenzhen Nanshan People's Hospital, Shenzhen, Guangdong, P.R. China  
2 Department of Neurosurgery, The First Affiliated Hospital of Xinjiang Medical University, Urumqi, Xinjian, P.R. China  
3 Department of Mental Health, Shenzhen Futian Hospital for Chronic Diseases, Shenzhen, Guangdong, P.R. China  
4 Department of Emergency, Dongying District People's Hospital, Dongying, Shandong, P.R. China  
5 Department of Radiology, Shenzhen Nanshan People's Hospital, Shenzhen, Guangdong, P.R. China

**Corresponding Author:**  
**Source of support:**

\* Mei Jiang and Xin Shi contributed equal  
Wu Wei, e-mail: [doc\\_wuwei21@sina.com](mailto:doc_wuwei21@sina.com)  
This work was supported by Medical Scientific Research Foundation of Guangdong Province of China (A2017576)

**Background:** Medullary thyroid carcinoma (MTC), a rare type of thyroid cancer, is a big challenge in clinical treatment. However, the pathogenesis of MTC remains poorly understand. MicroRNAs (miRNAs) were previously demonstrated to be involved in the pathogenesis of MTC, however, the roles of majority of miRNAs in MTC are still undetermined.





**Material/Methods:** Two GEO miRNA expression profiles (GSE40807, GSE97070) were downloaded, and the differentially expressed miRNAs (DEmiRNAs) of GSE40807 and GSE97070 were analyzed by bioinformatics methods. Expressions of miRNAs were detected by quantitative real-time polymerase chain reaction; cell proliferation was examined through Cell Counting Kit-8, colony formation and *in vivo* tumor growth assays; the interaction between miRNA and mRNA was verified by dual-luciferase reporter assay; functional analysis of target genes was performed using the Database for Annotation, Visualization and Integrated Discovery (DAVID, [www.david.ncifcrf.gov](http://www.david.ncifcrf.gov)) software.

**Results:** Ten miRNAs were identified to be dysregulated in both GSE40807 and GSE97070 datasets, and miR-31-3p showed the highest change fold (Log fold change=-3.460625 in GSE40807 and Log fold change=-0.07084374 in GSE97070). MiR-31-3p expression was significantly downregulated in MTC, and low miR-31-3p expression showed a poor prognosis relative to high miR-31-3p expression ( $P<0.05$ ). Functionally, miR-31-3p inhibited MTC cell proliferation *in vitro* and *in vivo*. Functional analysis also showed that the target genes of miR-31-3p were involved in numerous of biochemical processes and pathways, of which Ras signaling pathway was selected for further study. RASA2, overexpressed in MTC, were negatively regulated by miR-31-3p. In addition, we found that knockdown of RASA2 inhibited MTC cell proliferation.

**Conclusions:** Reduced expression level of miR-31-3p might play a key role in the tumorigenesis of MTC by targeting critical pathways, especially Ras signaling pathway.

**MeSH Keywords:** **Carcinoma, Medullary • Gene Targeting • MicroRNAs**

**Full-text PDF:** <https://www.medscimonit.com/abstract/index/idArt/916815>

 3043  —  5  45



## Background

Thyroid cancer ranks the first in the most prevalence cancer in endocrine system, accounting for more than 95% of all endocrine cancer incidence in 2017 in the United State [1]. According to the estimation of the American Cancer Society, there will be 52 070 new cases of and 2170 deaths from thyroid cancer in the United State in 2019 [2]. Papillary thyroid cancer (PTC), follicular thyroid cancer (FTC), poor differentiated thyroid cancer (PDTC), and anaplastic thyroid cancer (ATC), derived from follicular cells, are considered to be the most common four types of thyroid cancer that accounts for approximately 90% of all thyroid cancer cases [3–5]. Medullary thyroid carcinoma (MTC) is a rare type of thyroid cancer, representing for 5–10% of all cases [6]. Unlike the 4 common types of thyroid cancer, MTC primarily originates from parafollicular cells and frequently exhibit intermediate malignant degree [7]. According to the pathogenesis, MTC can be further divided as hereditary form (accounts for 25% of MTC) and sporadic form (accounts for 75% of MTC) [8]. The hereditary form could be curable if it is diagnosed at an early clinical stage and prophylactic total thyroidectomy is applied [9,10]. However, the sporadic form often exhibits more extensive symptoms and more unpromising prognosis than hereditary form [11]. Although MTC is a rare type of neuroendocrine malignancies with an incidence of around 0.21 cases in 100 000 person a year, it is very difficult to treat, especially for those advanced MTC patients with distant metastasis [12].

MicroRNAs (miRNAs), characterized by short length (~22 nucleotides), are a key subtype of non-coding RNAs that involved in the regulation of post-transcription [13,14]. It was well documented that miRNAs could silence the expression levels of corresponding genes by binding to the 3' untranslated region (UTR) region of target mRNAs [15]. Increasing evidence has shown that miRNAs participated in multiple biological processes, which were associated with the initiation and progression of tumors, such as tumor cell proliferation, metastasis, invasion, and apoptosis [15,16]. Up until now, miRNAs were demonstrated to be involved in almost all kinds of human tumors including breast cancer, lung cancer, and liver cancer [17–19]. The roles of miRNAs in MTC were also investigated by numerous of studies [20,21], however, a large proportion of miRNAs have not been well studied.

To identify MTC-associated miRNAs, we analyzed the differentially expressed miRNAs (DEmiRNAs) in 2 GSE datasets (GSE40807 and GSE97070) using bioinformatics analysis in this study. Among the 10 miRNAs dysregulated in both GSE40807 and GSE97070, miR-31-3p showed the highest change fold. Previous studies have shown that miR-31-3p plays a key role in multiple human cancers, such as colorectal cancer, oral cancer, and cervical cancer [22–24]. However, whether miR-31-3p

involves in the pathogenesis of MTC remains largely unclear. The present study aims to investigate the biological functions of miR-31-3p in MTC, and attempts to reveal the underlying molecular mechanisms.

## Material and Methods

### MTC tissue samples and cell lines

A total of 22 pairs of MTC and para-carcinoma tissues of MTC patients were collected in our study from the Shenzhen Nanshan People's Hospital. Informed consents were obtained from all participants that involved in this study, and the manipulates were approved by the ethics committee of Shenzhen Nanshan People's Hospital. The immortalized normal thyroid follicular cell line NThy-ori-3.1 and human MTC cell lines (TT) were all provided by the American Type Culture Collection (ATCC, Manassas, VA, USA); MTC cell lines (MZ-CRC-1) were purchased from BeNa Culture Collection (Kunshan, China; BNCC341849). All cells were maintained in the RPMI-1640 (Gibco, Thermo Fisher Scientific, Inc., Waltham, MA, USA) containing 10% fetal bovine serum (FBS) under the condition of 37°C and 5% CO<sub>2</sub>.

### Microarray datasets

The miRNA datasets (GSE40807 and GSE97070) were searched and downloaded from the GEO database (<https://www.ncbi.nlm.nih.gov/geo/>). GSE40807 was conducted through GPL8227 platforms (Agilent-019118 Human miRNA Microarray 2.0 G4470B) and consisted of 80 samples. GSE97070 was conducted by GPL18402 platforms (Agilent-046064 Unrestricted Human miRNA V19.0 Microarray) and consisted of 20 samples. Differentially expressed miRNAs (DEmiRNAs) between normal and MTC samples were screened based on the 2 GSE datasets, respectively. The volcano plots of DEmiRNAs was conducted via Morpheus (a web-based tool, <https://software.broadinstitute.org/morpheus/>).

### RNA extraction and quantitative real-time PCR (RT-PCR) assay

Total RNAs of treated MTC clinical tissue samples and cell lines were prepared using the TRIzol reagent (Invitrogen, Carlsbad, CA, USA) under the instruction of manufacturer. Quality of extracted RNAs were examined by NanoDro2000c (Thermo Scientific, Waltham, USA). Next, 2 µg of extracted total RNAs were used for cDNA synthesis with BestarTM qPCR RT kit (#2220, DBI Bioscience, China). RT-PCR was conducted on the ABI 7500 system (ABI Biosystems, USA) using BestarTM qPCR MasterMix (#2043, DBI Bioscience, China). The sequence of primers used in this study was as follow: GAPDH, F: 5'-TGTCGTCATGGGTGTAAC-3',

R: 5'-ATGGCATGGACTGTGGTCAT-3';  
 U6, F: 5'-GCTTCGGCAGCACATATACTAAAAT-3',  
 R: 5'-CGCTTCACGAATTTGCGTGCAT-3';  
 miR-31-3p, F: 5'-ACACTCCAGCTGGGTGCTATGCCAACAT-3',  
 R: 5'-TGGTGTCTGGAGTTCG-3';  
 RASA1, F: 5'-CACCACCAGAGCCAGTAGAA-3',  
 R: 5'-CGGCCACCTCTTCTACTAG-3';  
 RASA2, F: 5'-GCTACCCGATGTCTGGATGA-3',  
 R: 5'-ATTACAGTGGGGCAGCTCAT-3';  
 RASA4, F: 5'-GACTTCTGGACCTGCTCTT-3',  
 R: 5'-GTCCAGCTCCACGTACTTCT-3'.

The expression of RASA1, RASA2, and RASA4 were normalized to GAPDH, miR-31-3p was normalized to U6, and gene expression was quantified via  $2^{-\Delta\Delta Ct}$  method.

### RNA transfection

MiR-31-3p mimic and its negative control (mimic control), as well as RASA2 siRNAs (si-RASA2) and its negative control (si-NC), were all designed and purchased from the GenePharma (China). For cell transfection, MTC cells were seeded into 96-well plates and maintained at 37°C overnight followed by the transfection of corresponding RNAs with the Lipofectamine 3000 (Invitrogen) following the manufacturer's instructions.

### Cell Counting Kit-8 (CCK-8) assay

Cell viability of treated MTC cell lines was assessed via the Cell Counting Kit-8 (CCK-8) (Dojindo, Rockville, MD, USA) according to the protocols provided by the manufacturers. Briefly, treated MTC cells were collected and plated into 96-well plates at a concentration of  $3 \times 10^4$  cells/well and cultured at 37°C overnight. Next, CCK-8 solution (10  $\mu$ L) was added into each well and incubated for 10 minutes. Finally, the absorbance value of each well was detected with a microplate reader at 450 nm at 0, 12, 24, 48 and 72 hours.

### Colony formation assay

Cell proliferation of treated MTC cells was evaluated via colony formation assay. In brief, after treating with corresponding RNAs, MTC cells were seeded into 6-well plates at a density of 3000 cells/well and maintained for 2 weeks at 37°C in a cell incubator with 5% CO<sub>2</sub> and 95% O<sub>2</sub>. Next, formed cell colonies were fixed by 4% paraformaldehyde and stained with Giemsa solution for 30 minutes, respectively. The visible colonies were counted manually.

### In vivo tumor growth assay

For *in vivo* tumorigenicity, BALB/c-nude mice (4-week-old, n=20) were randomly divided into 2 groups with 10 mice in each group. Then, TT cells transfected with miR-31-3p or mimic

control were harvested and re-suspended in RPMI-1640 medium, making the final concentration  $1 \times 10^5$  cells/mL. We then subcutaneously injected nude mice with 200  $\mu$ L TT cell suspensions into the left flank of body. Tumor volume and weight were detected.

### Functional analysis

The Database for Annotation, Visualization and Integrated Discovery (DAVID, [www.david.ncifcrf.gov](http://www.david.ncifcrf.gov)) software, integrates the Gene Ontology (GO) and Kyoto Encyclopedia of Genes and Genomes (KEGG) databases, was applied to explore the functional role of miR-31-3p target genes. The enrichment values of GO terms and KEGG pathways were assessed through Fisher's exact test.

### Dual luciferase reporter assay

The interaction between miR-31-3p and RASA2 was verified by dual-luciferase reporter assay in TT and MZ-CRC-1 cells. For the establishment of recombinant plasmids, the wild type (WT) and mutant (mut) fragments of RASA2 3'-UTR containing putative miR-31-3p binding sites were inserted into the pGL3 (Promega, USA) vector to form recombinant luciferase plasmids: RASA2 3'-UTR-WT and RASA2 3'-UTR-mut. For dual-luciferase reporter assay, TT and MZ-CRC-1 cells ( $2 \times 10^5$  cells/well) were seeded into 96-well plates and cultured at 37°C overnight. Subsequently, TT and MZ-CRC-1 cells were co-transfected with miR-31-3p or mimic control and RASA2 3'-UTR-WT or RASA2 3'-UTR-mut. The firefly and Renilla luciferase activities of treated TT and MZ-CRC-1 cells were examined using the Dual-Luciferase Assay System (Promega), and Renilla luciferase activity was normalized to firefly luciferase activity.

### Statistical analysis

Data were expressed as mean  $\pm$ SEM in this study, One-way analysis of variance, conducted using SPSS v20 software (IBM Corp., Armonk, NY, USA), was applied to compare the difference between groups, P value less than 0.05 was considered as significant.

## Results

### MiR-31-3p was identified to be downregulated in MTC

To identify miRNAs that might be involved in the pathogenesis of MTC, 2 miRNA profiles (GSE40807 and GSE97070) were downloaded from the GEO database ([www.ncbi.nlm.nih.gov/geo](http://www.ncbi.nlm.nih.gov/geo)). Volcano plots were formed to show the differentially expressed miRNAs in GSE40807 and GSE97070 datasets through R software (Figure 1A, 1B). Ten miRNAs (miR-31-3p, miR-455-5p,

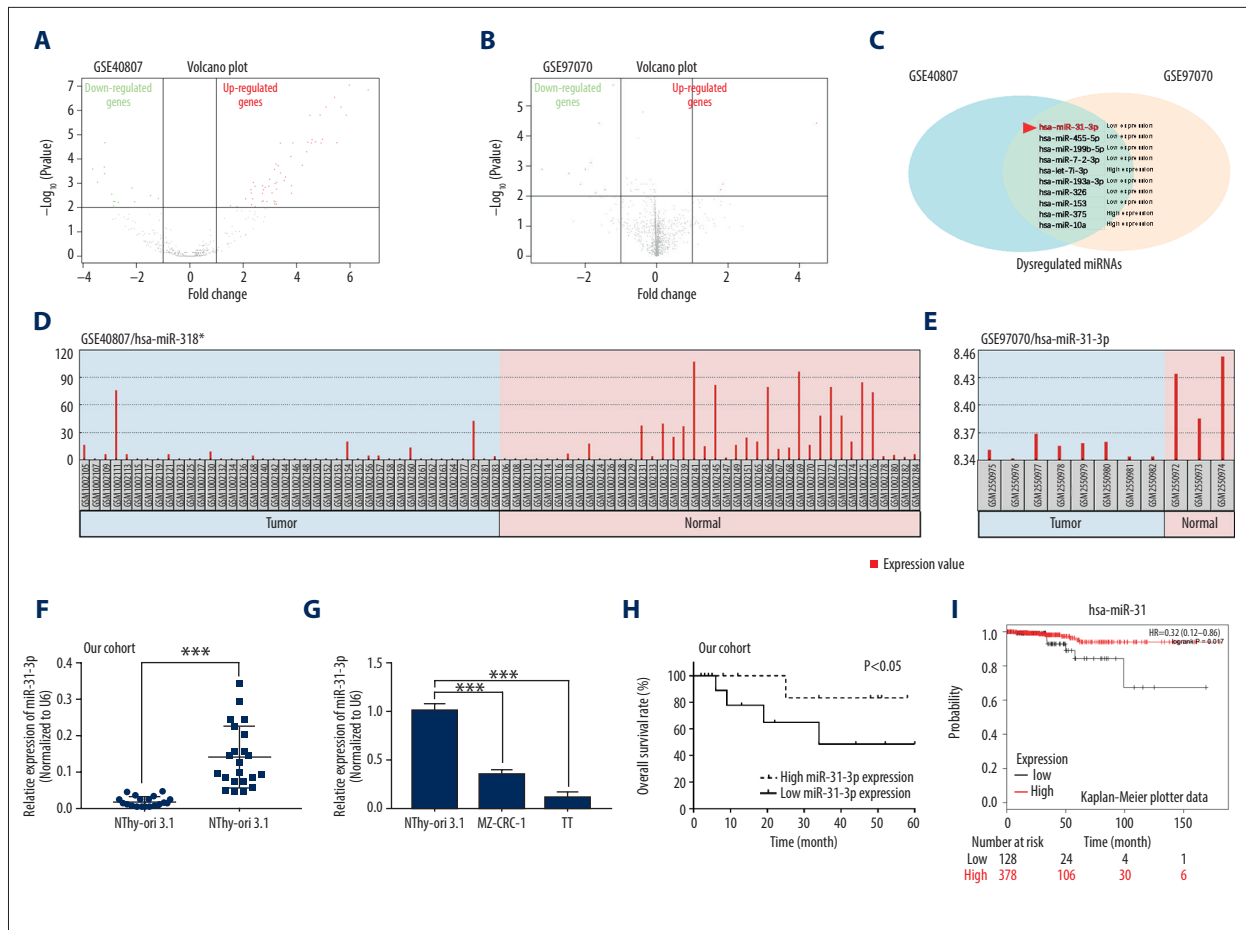


**Figure 1.** MiR-31-3p was identified to be downregulated in medullary thyroid carcinoma (MTC). (A, B) Volcano plot of dysregulated miRNAs in GSE40807 or GSE97070. (C) Venn diagram exhibiting the miRNAs that were dysregulated in both GSE40807 and GSE97070 datasets. (D, E) GEO2R analysis showing the expression of miR-31-3p in MTC and normal samples from GSE40807 and GSE97070 datasets. (F) Relative expression of miR-31-3p of 22 pairs of MTC and para-carcinoma tissues were detected by quantitative real-time polymerase chain reaction. (G) Expression of miR-31-3p was examined in 1 immortalized normal thyroid follicular cell line NThy-ori-3.1 and 2 human MTC cell lines MZ-CRC-1 and TT. (H) Overall survival rate of MTC patients with high or low miR-31-3p expression. (I) Kaplan-Meier plots showing overall survival in MTC patients with high or low miR-31-3p expression.

miR-199b-5p, miR-7-2-3p, let-7i-3p, miR-193a-3p, miR-326, miR-153, miR-375, and miR-10a) were found to be both dysregulated in GSE40807 and GSE97070 datasets (Figure 1C). GEO2R analysis of the 10 dysregulated miRNAs indicated that miR-31-3p was lowly expressed in MTC tissue samples compared to normal samples in GSE40807 and GSE97070 datasets (Figure 1D, 1E). To confirm the downregulation of miR-31-3p, we then examined its expression in both MTC clinical tissue samples and cell lines by qRT-PCR. As results indicated that miR-31-3p expression was significantly downregulated in MTC tissues (n=22) compared to para-carcinoma tissues (n=22), ( $P < 0.001$ , Figure 1F). Moreover, compared to the immortalized normal thyroid follicular cell line NThy-ori-3.1, miR-31-3p expression was significantly reduced in 2 MTC cell lines MZ-CRC-1 and TT ( $P < 0.001$ , Figure 1G). In addition, data

from clinical practice and Kaplan-Meier Plotter data showed that MTC patients with high miR-31-3p expression (n=11) exhibited a better prognosis than those patients with low miR-31-3p (n=11), ( $P < 0.05$ , Figure 1H, 1I).

### Overexpression of miR-31-3p inhibited MTC cell proliferation *in vitro* and *in vivo*

To investigate the biological functions of miR-31-3p in MTC, we overexpressed its expression in TT and MZ-CRC-1 cells followed by the analysis of cell proliferation using CCK-8, colony formation and *in vivo* tumor growth assays. As qRT-PCR results showed that miR-31-3p mimic treatment significantly increased miR-31-3p expression in TT and MZ-CRC-1 cells ( $P < 0.05$ , Figure 2A). For CCK-8 assay, cell viability of TT and

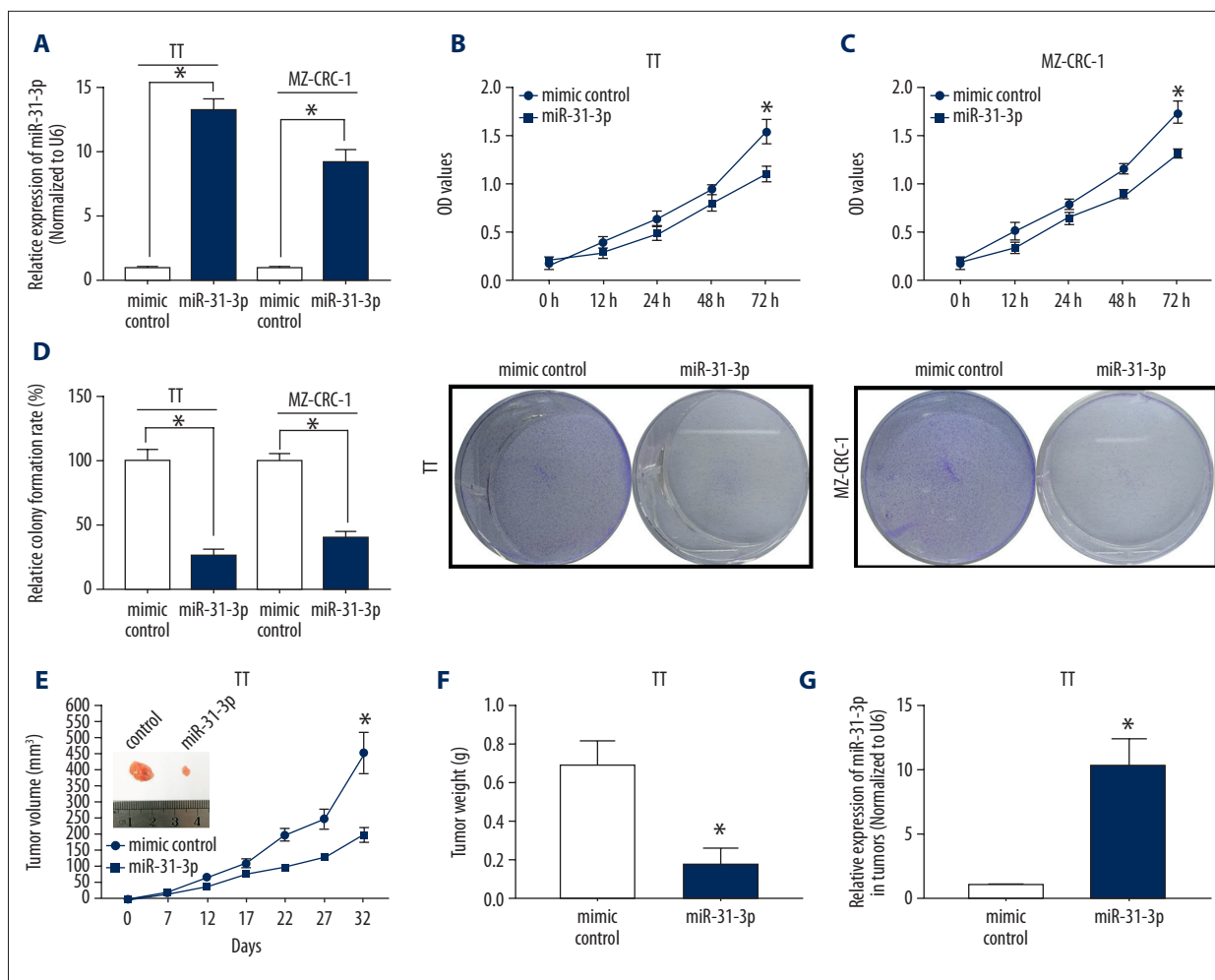


**Figure 2.** Overexpression of miR-31-3p inhibited medullary thyroid carcinoma (MTC) cell proliferation *in vitro* and *in vivo*. (A) Overexpression efficiency of miR-31-3p in 2 human MTC cell lines MZ-CRC-1 and TT was examined by quantitative real-time polymerase chain reaction. (B, C) Effects of miR-31-3p overexpression on viability of TT and MZ-CRC-1 cells were evaluated through Cell Counting Kit-8 assay. (D) Colony formation assay was performed to assess the proliferation of TT and MZ-CRC-1 cells treated with miR-31-3p mimics or mimic control. (E) Nude mice (n=20) were injected with TT cells transfected with miR-31-3p or negative control (NC) followed by the detection of tumor volume after 0, 7, 12, 17, 22, 27, and 32 days after injection. (F) The weight of tumor isolated from mice injected with miR-31-3p overexpressed TT cells. (G) Relative miR-31-3p expression of MTC tumor formed by miR-31-3p mimic or its control transfected TT cells.

MZ-CRC-1 cells transfected with miR-31-3p was significantly inhibited compared to those cells transfected with mimic control ( $P < 0.05$ , Figure 2B, 2C). For colony formation assay, the colony number was lower in the miR-31-3p transfected TT and MZ-CRC-1 cells than those mimic control transfected cells ( $P < 0.05$ , Figure 2D). For *in vivo* tumor growth assay, TT cells transfected with miR-31-3p or mimic control were subcutaneously injected into the left flank of nude mice, the tumor volume and weight were remarkably suppressed in miR-31-3p group (n=10) than mimic control group (n=10), ( $P < 0.05$ , Figure 2E, 2F). Moreover, the expression of miR-31-3p was higher in the xenograft formed by miR-31-3p transfected TT cells than that formed by mimic control transfected TT cells ( $P < 0.05$ , Figure 2G).

### GO and KEGG analysis of miR-31-3p target genes

Bioinformatics methods were used to analyze the functions of miR-31-3p based on its target genes ([http://www.targetscan.org/vert\\_72/](http://www.targetscan.org/vert_72/)). GO analysis was carried out to assess target gene enrichments in terms of biological process (BP), cellular component (CC) and molecular function (MF). Under BP, the top 10 GO terms were “negative regulation of T cell proliferation”, “negative regulation of leukocyte proliferation”, “negative regulation of mononuclear cell proliferation”, “negative regulation of lymphocyte proliferation”, “negative regulation of lymphocyte activation”, “gland development”, “negative regulation of cell activation”, “negative regulation of T cell activation”,

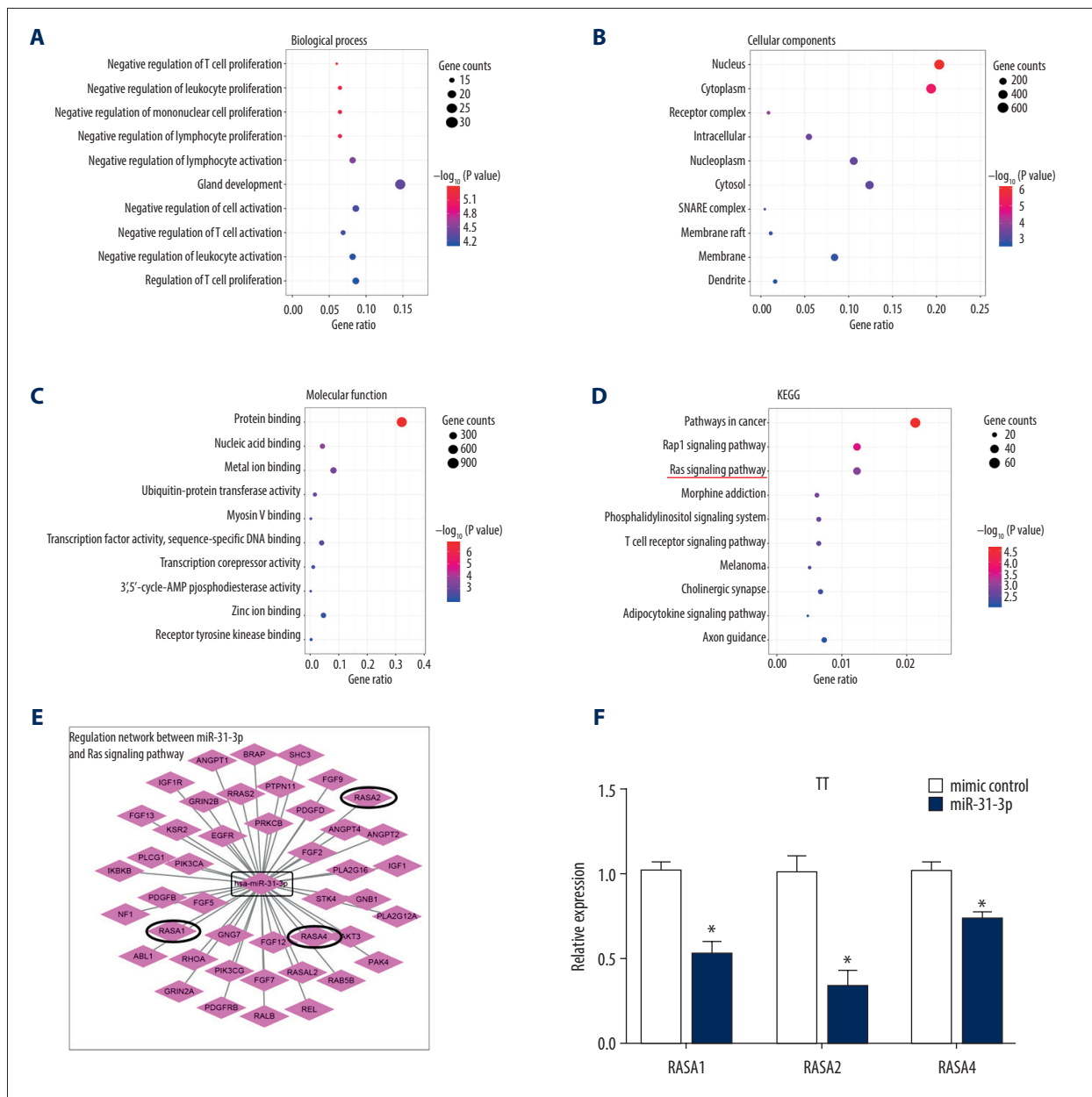


**Figure 3.** Gene Ontology (GO) and Kyoto Encyclopedia of Genes and Genomes (KEGG) database analysis of miR-31-3p target genes. (A) Biological process. (B) Cellular components. (C) Molecular function. (D) KEGG. (E) Regulation network between miR-31-3p and Ras signaling pathway. (F) Relative expression levels of RASA1, RASA2 and RASA4 of TT cells transfected with miR-31-3p mimic or its control were measured by quantitative real-time polymerase chain reaction.

“negative regulation of leukocyte activation”, and “regulation of T cell proliferation” (Figure 3A). Under CC, the top 10 GO terms were “nucleus”, “cytoplasm”, “receptor complex”, “intracellular”, “nucleoplasm”, “cytosol”, “snare complex”, “membrane raft”, “membrane”, and “dendrite” (Figure 3B). Under MF, the top 10 GO terms were “protein binding, nucleic acid binding”, “metal ion binding”, “ubiquitin-protein transferase activity”, “myosin v binding”, “transcription factor activity, sequence-specific DNA binding”, “transcription corepressor activity”

activity”, “3',5'-cyclic-AMP phosphodiesterase activity”, “zinc ion binding” and “receptor tyrosine kinase binding” (Figure 3C). KEGG analysis revealed the top 10 pathways, which include “pathways in cancer”, “Rap1 signaling pathway”, “ras signaling pathway”, “morphine addiction”, “phosphatidylinositol signaling system”, “T cell receptor signaling pathway”, “melanoma”, “cholinergic synapse”, “adipocytokine signaling pathway” and “axon guidance” (Figure 3D). We then focused our interesting in the regulation network between miR-31-3p and Ras

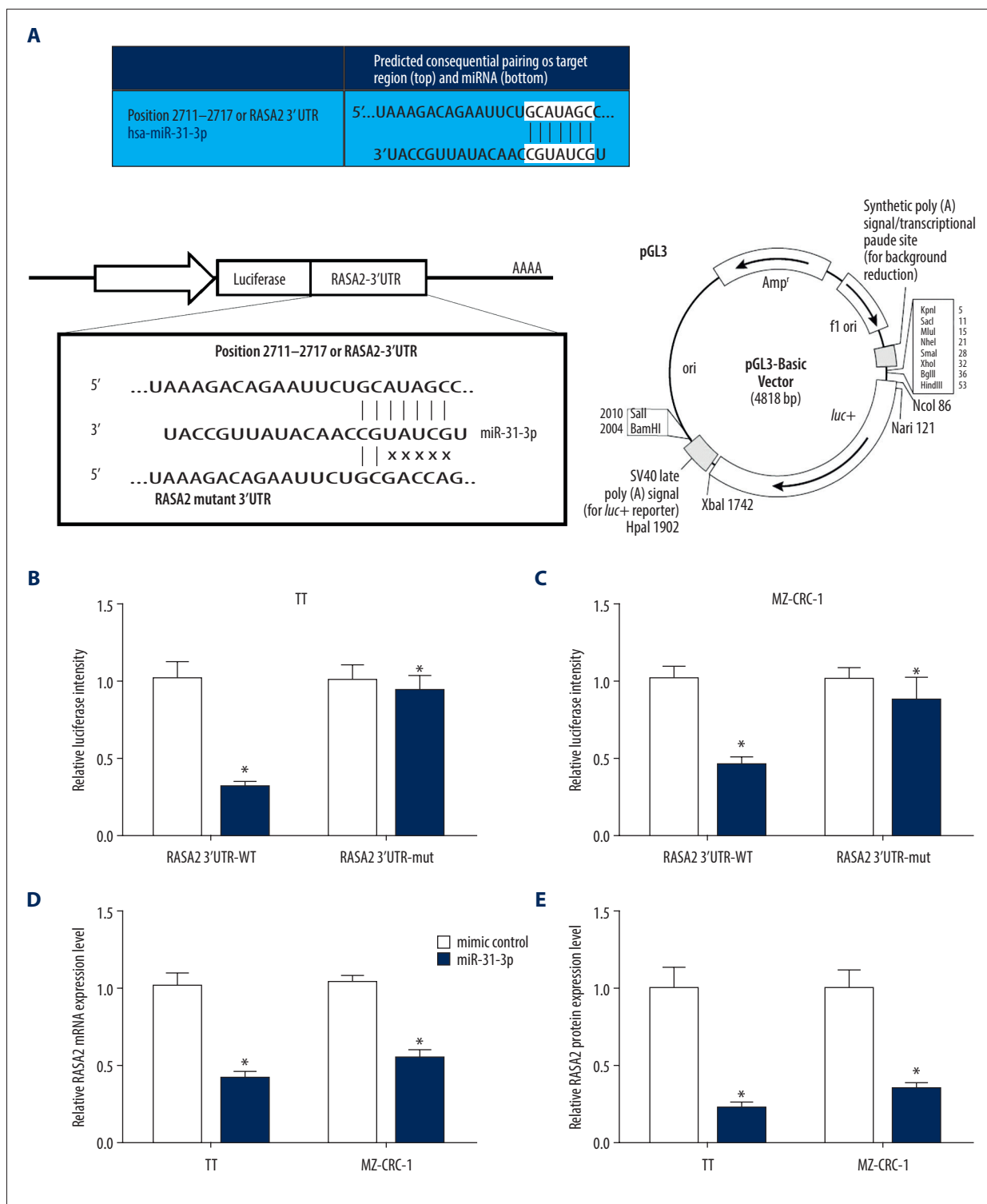


**Figure 4.** MiR-31-3p negatively regulated RASA2 by directly bind to it. **(A)** The predicted consequential pairing of target region of RASA2 and miR-31-3p, and the schematic diagram of establishment of luciferase recombinant plasmid. **(B, C)** Dual-luciferase reporter assay was performed in 2 human MTC cell lines MZ-CRC-1 and TT to verify the interaction between miR-31-3p and RASA2. **(D, E)** Relative RASA2 mRNA and protein expression in TT and MZ-CRC-1 cells treated with miR-31-3p mimic or control.

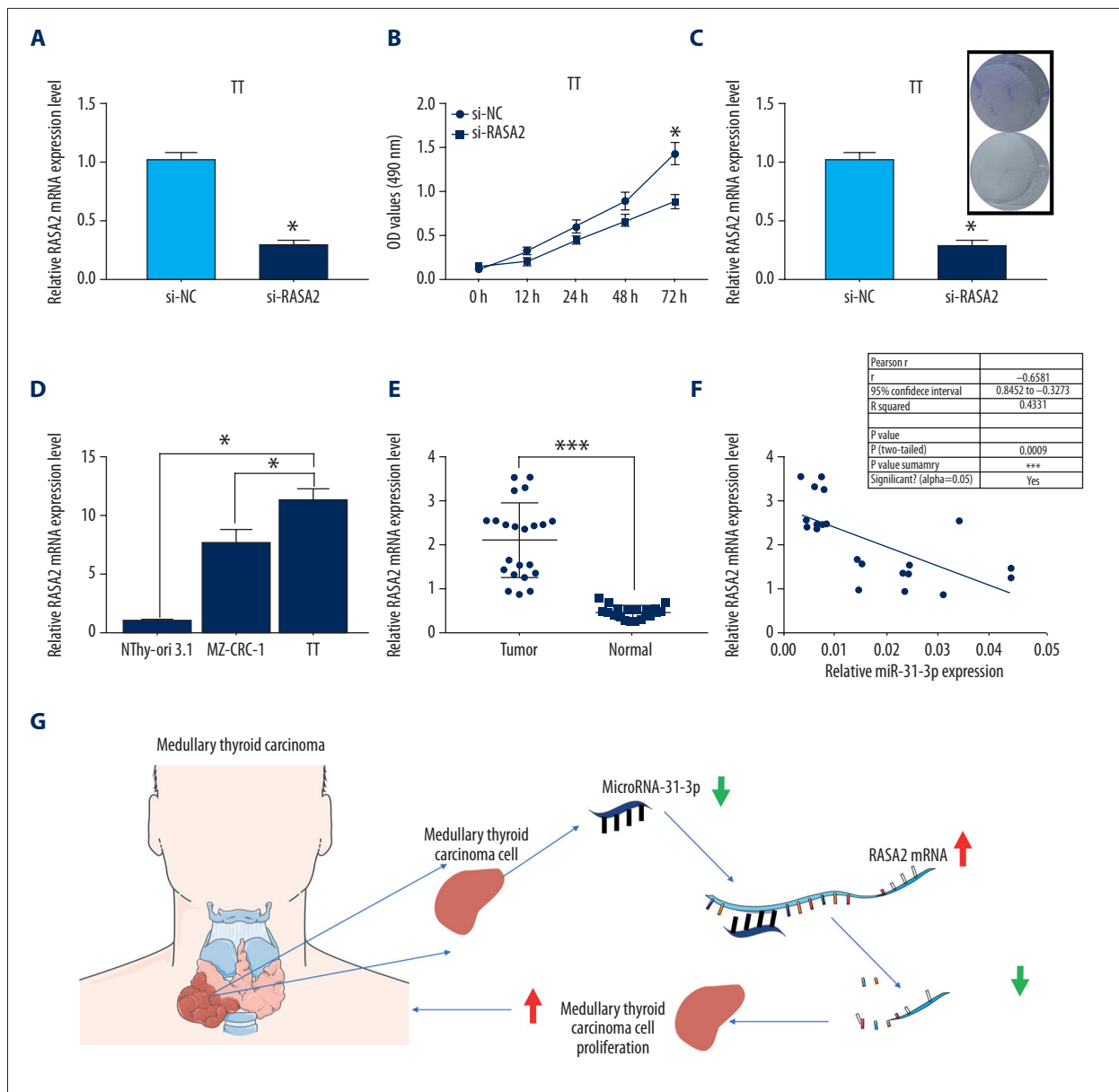


**Figure 5.** Knockdown of RASA2 suppressed medullary thyroid carcinoma (MTC) cell proliferation *in vitro*. (A) Knockdown efficiency of si-RASA2 in human MTC cell line TT was determined by quantitative real-time polymerase chain reaction (qRT-PCR). (B) Cell Counting Kit-8 analysis of TT cell viability was performed in si-NC or si-RASA2 treated TT cells. (C) Colony formation assay was carried out to evaluate the effects of si-RASA2 on cell proliferation of TT cells. (D) Relative expression of RASA2 was examined by qRT-PCR in immortalized normal thyroid follicular cell line NThy-ori-3.1, and 2 human MTC cell lines MZ-CRC-1 and TT. (E) Relative miR-31-3p expression was assessed in 22 pairs MTC and para-carcinoma tissues. (F) Correlation between the expression levels of RASA2 and miR-31-3p in MTC tissue samples (n=22). (G) Schematic diagram of the underlying molecular mechanism of miR-31-3p in the pathogenesis of MTC.

signaling pathway (Figure 3E). In the following experiments, we found that overexpression of miR-31-3p could significantly downregulated the mRNA expression levels of RASA1, RASA2, and RASA4 in TT cells ( $P<0.05$ , Figure 3F).

#### miR-31-3p negatively regulated RASA2 by directly bind to it

Since RASA2 was demonstrated by bioinformatics analysis to possess the complementary sequence of miR-31-3p in its 3'-UTR regions (Figure 4A, upper panel), we speculated that



miR-31-3p might bind to RASA2. Dual luciferase reporter assay was used to assess the interaction between miR-31-3p and RASA2 in TT and MZ-CRC-1 cells. The fragments of wild type and mutant RASA2 3'-UTR containing miR-31-3p binding sites were inserted into the pGL3 vector to form recombinant luciferase plasmids: RASA2 3'-UTR-WT and RASA2 3'-UTR-mut (Figure 4A, lower panel). For dual luciferase reporter assay, we found that miR-31-3p, but not mimic control, significantly attenuated the luciferase activity of TT and MZ-CRC-1 cells driven by RASA2 3'-UTR-WT ( $P < 0.05$ , Figure 4B, 4C). The luciferase activity of TT and MZ-CRC-1 cells driven by RASA2 3'-UTR-mut was not affected by miR-31-3p and mimic control ( $P < 0.05$ , Figure 4B, 4C). In addition, we examined the expression of RASA2 in miR-31-3p overexpressed or knockdown TT and MZ-CRC-1 cells by qRT-PCR. As results indicated that miR-31-3p overexpression of TT and MZ-CRC-1 cells significantly decreased the expression of RASA2 ( $P < 0.05$ , Figure 4D, 4E).

### Knockdown of RASA2 suppressed MTC cell proliferation *in vitro*

To understand the roles of RASA2 in MTC, we transfected TT cells with si-RASA2 to silence the expression of RASA2 followed by the analysis of CCK-8 and colony formation assays. Knockdown efficiency of si-RASA2 in TT cells was verified by qRT-PCR ( $P < 0.05$ , Figure 5A). For CCK-8 assay, cell viability of si-RASA2 transfected TT cells was significantly inhibited compared to si-NC transfected TT cells ( $P < 0.05$ , Figure 5B). For colony assay, the colony number was significantly reduced in si-RASA2 transfected TT cells compared to si-NC transfected TT cells ( $P < 0.05$ , Figure 5C). These findings suggested that knockdown of RASA2 suppressed MTC cell proliferation *in vitro*. Moreover, we found that RASA2 expression of MZ-CRC-1 and TT cells was higher than that of NThy-ori-3.1 cells ( $P < 0.05$ , Figure 5D). Compared to para-carcinoma tissues ( $n=22$ ), RASA2 expression was significantly increased in MTC tissue samples ( $n=22$ ), ( $P < 0.001$ , Figure 5E). In addition, we found a negative correlation between the expression levels of miR-31-3p and RASA2 in MTC tissue samples ( $n=22$ ,  $P < 0.001$ ,  $r^2=0.4331$ , Figure 5F). Taken together, knockdown of miR-31-3p promoted MTC cell proliferation by upregulating RASA2 mRNA (Figure 5G).

## Discussion

MiRNAs were previously found to be dysregulated in various of human tumor tissues compared to para-carcinoma tissues, indicating an important role of miRNAs in the tumorigenesis of human tumor. Previous researches have shown that miRNAs participated in the progress of MTC, such as miR-153-3p [25], miR-224 [26], miR-9-3p [27] and miR-375 [28], etc. However, the expression profile of miRNAs in MTC was not well studied up until now, the majority of studies have focused on a

limited number of miRNAs using qRT-PCR. To our best knowledge, the first array-based miRNAs profile analysis of MTC was performed by Nikiforova et al. in 2008, which only included 2 MTC samples [29]. Until recently, large scale miRNAs expression profile analysis was carried out [30,31]. In this study, we performed a miRNA microarray profiling in 2 GSE datasets (GSE40807 or GSE97070), which were searched and downloaded from the GEO database ([www.ncbi.nlm.nih.gov/geo](http://www.ncbi.nlm.nih.gov/geo)). We identified a signature of miRNAs that dysregulated in MTC tissue samples compared to normal samples of both GSE40807 or GSE97070 datasets, including those have already recognized by other studies: miR-193a-3p [32], miR-375 [33] and miR-10a [34], together with a novel set of miRNAs that unrevealed: miR-31-3p, miR-455-5p, miR-199b-5p, miR-7-2-3p, let-7i-3p, miR-326, and miR-153. Among these unreported miRNAs, miR-31-3p showed the highest change fold in MTC samples compared to normal samples. We, therefore, selected miR-31-3p for the further study.

MiR-31-3p has been reported to be associated with the initiation and progression of multiple human cancers, of which colorectal cancer exhibited the most well studied [22,35]. For instance, results from a miRNAs profiling that performed in a set of 87 patients with metastatic colorectal cancer (mCRC) refractory to chemotherapy treated with anti-EGFR antibodies showed that miR-31-3p might be a novel mCRC biomarker for the diagnosis of patients with wild-type KRAS mCRC who are more likely to respond to anti-EGFR therapy [36]. However, to our best knowledge, the roles of miR-31-3p in MTC remain undetermined. In our study, we found a significant downregulation of miR-31-3p in MTC tissues and cell lines. Overexpression of miR-31-3p significantly suppressed MTC cell proliferation *in vitro* and *in vivo*. These findings suggested that miR-31-3p might act as a tumor suppressor of MTC.

After determining the biological functions of miR-31-3p in MTC, we, subsequently, performed functional analysis to predict the molecular mechanisms underlying miR-31-3p. Multiple cellular signaling pathways were reported to be dysregulated in MTC, such as Ras/mammalian target of rapamycin (mTOR) pathway, PI3K-AKT-mTOR pathway,  $\beta$ -Catenin pathway and NF- $\kappa$ B pathway [37]. In the top 10 associated pathways predicted by KEGG analysis, Ras signaling pathway was selected for the further study. RAS protein is a binary switch that circulates between on and off states during signal transduction [38]. Mutations of RAS gene or its regulatory factors make RAS protein continuously active, which promotes the occurrence of disease [39]. Studies have shown that Ras pathway has significant effects in cell proliferation, differentiation, apoptosis and carcinogenic transformation [40,41]. At present, Ras has been reported to be a frequently mutated oncogene in a various of human cancers, including thyroid cancer, breast cancer, and lung cancer [42–44]. RASA2 serves as a GTPase activating protein (GAP)

regulating RAS, which is one of the most highly mutated oncogenes in cancer, while drugs targeting RAS have so far been ineffective [45]. Therefore, the role of RASA2 in cancer is crucial. In our study, RASA2 was identified to be bind and negatively regulated by miR-31-3p in MTC cells, and knockdown of RASA2 significantly inhibited MTC cell proliferation.

## References:

1. Siegel RL, Miller KD, Jemal A: Cancer Statistics, 2017. *Cancer J Clin*, 2017; 67(1): 7–30
2. Siegel RL, Miller KD, Jemal A: Cancer statistics, 2019. *Cancer J Clin*, 2019; 69(1): 7–34
3. Baloch ZW, LiVolsi VA: Special types of thyroid carcinoma. *Histopathology*, 2018; 72(1): 40–52
4. Azar FK, Lee SL, Rosen JE: Medullary thyroid cancer: An update for surgeons. *Am Surg*, 2015; 81(1): 1–8
5. Massimino M, Evans DB, Podda M et al: Thyroid cancer in adolescents and young adults. *Pediatr Blood Cancer*, 2018; 65(8): e27025
6. Barbet J, Campion L, Kraeber-Bodere F, Chatal JF, GTE Study Group: Prognostic impact of serum calcitonin and carcinoembryonic antigen doubling-times in patients with medullary thyroid carcinoma. *J Clin Endocrinol Metab*, 2005; 90(11): 6077–84
7. Weber T: Medullary thyroid carcinoma: Why is specialization mandatory? *Visc Med*, 2018; 34(6): 419–21
8. Leboulleux S, Baudin E, Travagli JP, Schlumberger M: Medullary thyroid carcinoma. *Clin Endocrinol (Oxf)*, 2004; 61(3): 299–310
9. Kebebew E, Ituarte PH, Siperstein AE et al: Medullary thyroid carcinoma: Clinical characteristics, treatment, prognostic factors, and a comparison of staging systems. *Cancer*, 2000; 88(5): 1139–48
10. Oczko-Wojciechowska M, Swierniak M, Krajewska J et al: Differences in the transcriptome of medullary thyroid cancer regarding the status and type of RET gene mutations. *Sci Rep*, 2017; 7: 42074
11. Qu N, Shi RL, Luo TX et al: Prognostic significance and optimal cutoff of age in medullary thyroid cancer. *Oncotarget*, 2016; 7(13): 15937–47
12. Randle RW, Balentine CJ, Levenson GE et al: Trends in the presentation, treatment, and survival of patients with medullary thyroid cancer over the past 30 years. *Surgery*, 2017; 161(1): 137–46
13. Tutar Y: MiRNA and cancer; Computational and experimental approaches. *Curr Pharm Biotechnol*, 2014; 15(5): 429
14. Tutar L, Ozgur A, Tutar Y: Involvement of miRNAs and pseudogenes in cancer. *Methods Mol Biol*, 2018; 1699: 45–66
15. Ors-Kumoglu G, Gulce-Iz S, Biray-Avci C: Therapeutic microRNAs in human cancer. *Cytotechnology*, 2019; 71(1): 411–25
16. Schwarzenbach H, Gahan PB: MicroRNA shuttle from cell-to-cell by exosomes and its impact in cancer. *Noncoding RNA*, 2019; 5(1): pii: E28
17. Malhotra P, Read GH, Weidhaas JB: Breast cancer and miR-SNPs: The importance of miR germ-line genetics. *Noncoding RNA*, 2019; 5(1): pii: E28
18. Hashemi ZS, Khalili S, Forouzandeh Moghadam M, Sadroddiny E: Lung cancer and miRNAs: A possible remedy for anti-metastatic, therapeutic and diagnostic applications. *Expert Rev Respir Med*, 2017; 11(2): 147–57
19. Zhao J, Fu Y, Wu J et al: The diverse mechanisms of miRNAs and lncRNAs in the maintenance of liver cancer stem cells. *Biomed Res Int*, 2018; 2018: 8686027
20. Chu YH, Hardin H, Schneider DF et al: MicroRNA-21 and long non-coding RNA MALAT1 are overexpressed markers in medullary thyroid carcinoma. *Exp Mol Pathol*, 2017; 103(2): 229–36
21. Shi L, Zhao SM, Luo Y et al: MiR-375: A prospective regulator in medullary thyroid cancer based on microarray data and bioinformatics analyses. *Pathol Res Pract*, 2017; 213(11): 1344–54
22. Laurent-Puig P, Grisoni ML, Heinemann V et al: Validation of miR-31-3p expression to predict cetuximab efficacy when used as first-line treatment in RAS wild-type metastatic colorectal cancer. *Clin Cancer Res*, 2019; 25(1): 134–41
23. Zeljic K, Jovanovic I, Jovanovic J et al: MicroRNA meta-signature of oral cancer: Evidence from a meta-analysis. *Ups J Med Sci*, 2018; 123(1): 43–49
24. Pedroza-Torres A, Fernandez-Retana J, Peralta-Zaragoza O et al: A microRNA expression signature for clinical response in locally advanced cervical cancer. *Gynecol Oncol*, 2016; 142(3): 557–65
25. Joo LJS, Weiss J, Gill AJ et al: RET kinase-regulated microRNA-153-3p improves therapeutic efficacy in medullary thyroid carcinoma. *Thyroid*, 2019; 29(6): 830–44
26. Cavedon E, Barollo S, Bertazza L et al: Prognostic impact of miR-224 and RAS mutations in medullary thyroid carcinoma. *Int J Endocrinol*, 2017; 2017: 4915736
27. Chen Y, Zhang S, Zhao R et al: Upregulated miR-9-3p promotes cell growth and inhibits apoptosis in medullary thyroid carcinoma by targeting BLCAP. *Oncol Res*, 2017; 25(8): 1215–22
28. Galuppini F, Bertazza L, Barollo S et al: MiR-375 and YAP1 expression profiling in medullary thyroid carcinoma and their correlation with clinical-pathological features and outcome. *Virchows Archiv*, 2017; 471(5): 651–58
29. Nikiforova MN, Tseng GC, Steward D et al: MicroRNA expression profiling of thyroid tumors: Biological significance and diagnostic utility. *J Clin Endocrinol Metab*, 2008; 93(5): 1600–8
30. Hudson J, Duncavage E, Tamburrino A et al: Overexpression of miR-10a and miR-375 and downregulation of YAP1 in medullary thyroid carcinoma. *Exp Mol Pathol*, 2013; 95(1): 62–67
31. Lassalle S, Zangari J, Popa A et al: MicroRNA-375/SEC23A as biomarkers of the *in vitro* efficacy of vandetanib. *Oncotarget*, 2016; 7(21): 30461–78
32. Santarpia L, Calin GA, Adam L et al: A miRNA signature associated with human metastatic medullary thyroid carcinoma. *Endocr Relat Cancer*, 2013; 20(6): 809–23
33. Romeo P, Colombo C, Granata R et al: Circulating miR-375 as a novel prognostic marker for metastatic medullary thyroid cancer patients. *Endocr Relat Cancer*, 2018; 25(3): 217–31
34. Mancikova V, Montero-Conde C, Perales-Paton J et al: Multilayer OMIC data in medullary thyroid carcinoma identifies the STAT3 pathway as a potential therapeutic target in RET(M918T) tumors. *Clin Cancer Res*, 2017; 23(5): 1334–45
35. Ramon L, David C, Fontaine K et al: Technical validation of a reverse-transcription quantitative polymerase chain reaction *in vitro* diagnostic test for the determination of MiR-31-3p expression levels in formalin-fixed paraffin-embedded metastatic colorectal cancer tumor specimens. *Biomark Insights*, 2018; 13: 1177271918763357
36. Manceau G, Imbeaud S, Thiebaut R et al: Hsa-miR-31-3p expression is linked to progression-free survival in patients with KRAS wild-type metastatic colorectal cancer treated with anti-EGFR therapy. *Clin Cancer Res*, 2014; 20(12): 3338–47

## Conclusions

Taken together, reduced miR-31-3p might acted as a tumor suppressor of MTC by binding and negative regulating the expression of RASA2, and thus affected the proliferation of MTC cell. Our findings not only enriched the underlying pathogenesis of MTC, but also provided a novel potential therapeutic pathway for MTC patients.

## Conflict of interest

None.

37. Giunti S, Antonelli A, Amorosi A, Santarpia L: Cellular signaling pathway alterations and potential targeted therapies for medullary thyroid carcinoma. *Int J Endocrinol*, 2013; 2013: 803171
38. Han CW, Jeong MS, Jang SB: Structure, signaling and the drug discovery of the Ras oncogene protein. *BMB Rep*, 2017; 50(7): 355–60
39. Bueno A, Morilla I, Diez D et al: Exploring the interactions of the RAS family in the human protein network and their potential implications in RAS-directed therapies. *Oncotarget*, 2016; 7(46): 75810–26
40. Xie L, Overbeek PA, Reneker LW: Ras signaling is essential for lens cell proliferation and lens growth during development. *Dev Biol*, 2006; 298(2): 403–14
41. Haigis KM, Kendall KR, Wang Y et al: Differential effects of oncogenic K-Ras and N-Ras on proliferation, differentiation and tumor progression in the colon. *Nat Genet*, 2008; 40(5): 600–8
42. Bockhorn M, Frilling A, Kalinin V et al: Absence of H- and K-ras oncogene mutations in sporadic medullary thyroid carcinoma. *Exp Clin Endocrinol Diabetes*, 2000; 108(1): 49–53
43. Liu R, Li J, Lai Y et al: Hsa-miR-1 suppresses breast cancer development by down-regulating K-ras and long non-coding RNA MALAT1. *Int J Biol Macromol*, 2015; 81: 491–97
44. Nkembo AT, Amisah F, Ntantie E et al: Polyisoprenylated cysteinyl amide inhibitors deplete K-Ras and induce caspase-dependent apoptosis in lung cancer cells. *Curr Cancer Drug Targets*, 2019 [Epub ahead of print]
45. Arafeh R, Qutob N, Emmanuel R, Keren-Paz A et al: Recurrent inactivating RASA2 mutations in melanoma. *Nat Genet*, 2015; 47(12): 1408–10